NASA
Technical Memorandum 107009

Army Research Laboratory
Technical Report ARL–TR–852

Experimental and Analytical Assessment of the Thermal Behavior of Spiral Bevel Gears

Robert F. Handschuh
Vehicle Propulsion Directorate
U.S. Army Research Laboratory
Lewis Research Center
Cleveland, Ohio

and

Thomas P. Kicher
Case Western Reserve University
Cleveland, Ohio

Prepared for the
1995 Fall Technical Meeting
sponsored by the American Gear Manufacturers Association
Charleston, South Carolina, October 16–18, 1995

National Aeronautics and
Space Administration

EXPERIMENTAL AND ANALYTICAL ASSESSMENT OF THE THERMAL BEHAVIOR OF SPIRAL BEVEL GEARS

Robert F. Handschuh
Army Research Laboratory
NASA Lewis Research Center
Cleveland, Ohio

Thomas P. Kicher
Case Western Reserve University
Cleveland, Ohio

Introduction:

In the design process of spiral bevel gears, the bending and contact stress calculations are made and repeated on until a satisfactory design is found based on the material capabilities and past experience. In many designs the thermal behavior or flash temperature calculation will not be made or even considered. However, in the design of aerospace spiral bevel gear meshes, this calculation can be just as important as those previously mentioned.

In aerospace applications such as that found in helicopters as shown in Fig. 1 [1], the gears are jet lubricated and the oil is then scavenged away to permit the highest operating efficiency. In applications such as helicopters the gears operate at high pitch line velocities and load such that the thermal behavior is of concern. A region of safe operation of a gear mesh can be found as shown in Fig. 2 [2,3]. Depending on the speed and load under which the gear mesh is operating, various regimes of different failure modes can be approached and even successful designs, if pushed to new operating conditions, can eventually reach a point where the thermal behavior can be of concern or cause failure.

The earliest work on the thermal behavior of gear systems, both experimental and analytical, dates back to the work of Blok [4,5]. Out of this work came the basis of which the "flash temperature" calculations are still made today. This work was further extended to spiral bevel and hypoid gears in the work of Coleman [6]. This methodology is still used to predict the flash temperature in a quick and efficient manner [7].

In the open literature, analytical work on the thermal behavior of spiral bevel gears is very limited. Other than the pioneering work of Ref. 6 only one other analytical study using a finite element based approach has been attempted [8] other than that of Refs. [9,10].

Experimental work is also very limited. Only the work of Refs. 11-13 have documented spiral bevel gear operating temperatures in an aerospace operating environment. Therefore an indepth study using experiments and analysis would be useful to characterize the thermal behavior of this type of gear system.

The objective of the research reported herein was to conduct an experimental and analytical study to characterize the thermal behavior of aerospace-quality spiral bevel gears. Experiments were conducted using thermocouples on spiral bevel pinions to measure bulk operating temperatures. Also, an infrared microscope was used to measure transient pinion surface temperatures at a position some rotational distance after meshing had occurred. An indepth analytical effort was undertaken. A finite element based approach was formulated using the actual gear geometry/gear design, tooth contact analysis, Hertzian contact analysis, and lubricant frictional behavior to apply the heat flux boundary conditions to the finite element model. The results from the experiments are compared to the analysis that was conducted.

NASA Test Apparatus:

The experimental results described in this study were attained using the Spiral Bevel Gear Test Rig located at NASA Lewis Research Center. A sketch of the overall facility which uses a closed-loop torque regenerative arrangement is shown in Fig. 3. Two sets of spiral bevel gears can be tested simultaneously in the arrangement used.

A cross-sectional view of the facility is shown in Fig. 4. Rotational motion is provided by v-belts from a 75 kW (100 hp) motor to a helical gear shaft that meshes with another helical gear that can move axially. Axial motion of the helical gear through a thrust piston permits the loop torque to be changed during facility operation. The shafting that is connected to the helical gears is also

driven at the same rotational speed as the gear member of the spiral bevel mesh. The right side of the test stand (slave side) operates with the gear driving the pinion and the left side operates in the normal manner with the pinion driving the gear. Both sides of the test stand however have contact on the normally contacting sides of the gear mesh, where the concave side of the pinion meshes with the convex side of the gear. The regenerative torque loop is closed through shafting and an in-the-loop, commercially available torquemeter. The operational capabilities of the test stand are given in Table 1 and the basic spiral bevel gear design specifications are provided in Table 2.

Thermal Measurement Instrumentation: Two methods to measure temperature were used in this study. The first type of measurement system involved the use of thermocouples that were imbedded or attached using an adhesive in four locations on the pinion member. An example of this is shown in Fig. 5. The four locations were the tooth top, root, toe, and heel. In all but the root locations the thermocouples were located approximately 0.76 mm (0.03 in.) below the machined boundaries. The thermocouple wiring was then connected to slip rings which transferred the signal to a laboratory computer. These measurements were for the bulk thermal properties of the pinion. As will be described later, in the analysis section, these locations are only exposed to steady state conditions once equilibrium is reached.

The second method used to investigate the thermal behavior of the pinion was the use of an infrared microscope system. A schematic of the system used is shown in Fig. 6. The infrared microscope has a sensor that responds to infrared radiation in the 1 to 10 mm range. The resultant voltage output of the sensor in the transient mode is related to the temperature difference of the surface under study, the surface emissivity, and the instrument calibration factor.

A clear line of sight is required to make this measurement and therefore must be made, in the study described herein, about 120° after the pinion had finished engagement with the gear. Also used with this measurement system is a proximity probe that tracked the pinion tooth location. Both of these signals were fed into a dual channel oscilloscope. This permitted the proper locating of the pinion active profile in the transient signal.

Experimental Results:

Thermocoupled Pinion: Three variations of test operating condition and arrangements for a number of conditions will now be described [9,13]. The effects of transmitted load, oil inlet temperature, and jet position (jet pressure) will be presented. All test data were taken after the measurements had stabilized with no change in temperature magnitude for a period of time, typically lasting 5 min.

First the effect of load at full speed on the four measured locations is shown in Fig. 7. The tooth top was always at a higher temperature than the tooth root, toe, and heel. The effect of going from approximately 50 to 100 percent load was a linear rise in the temperatures measured. The tooth top however increased at a higher rate than the other locations.

The second effect investigated was the effect of oil inlet temperature on the same four locations as was described earlier. Speed and load were both held constant at the 100 percent conditions of the facility while the oil inlet temperature was varied. Increasing the oil inlet temperature caused a nearly linear temperature increase in the four measurement locations as shown in Fig. 8. Note that the increase in the measured temperature was not as great as the change in the oil inlet temperature. Obviously the ambient convection conditions and the heat capacity of the attachment structure limited the response of the measured temperature to a fraction of the oil inlet temperature change.

The last set of data that will be discussed using the instrumented pinion will be the effect of jet orientation on the four measurement locations. The jet orientations are shown in Fig. 9. Five different positions of the lubricating jet were tested at two different lubricant jet flow rates (jet pressures). One jet position was tested at a time. Two locations of the lubricating jet produced similar and the lowest measured temperatures. Position 4 is the into-mesh position and Position 5 is the out-of-mesh position. Either of these produced the lowest indicated temperatures. Based on this, the out-of-mesh position would be chosen to maintain the highest system efficiency.

Lubricant jet flow rate had less of an effect at jet locations 1 to 3, but had a significant effect on temperature at locations 4 and 5. Therefore a substantial overall pinion operating temperature decrease could be produced at these locations (4 and 5) by increasing the lubricant flow rate.

Infrared Microscope Measurements: Measurements using an infrared microscope are very difficult to make in a gearbox because of the turbulent windage caused by the lubricant interacting with the meshing gear teeth. This windage permitted the measurement to be made at only a few jet positions. The results described in this report had the jet oriented 90° on the gear at either the into- or out-of-mesh position. The infrared microscope monitored the pinion under study.

When the infrared microscope is positioned, a single stationary region is examined with a diameter of approximately 0.25 mm (0.01 in.). As the pinion rotates by, the measurement location varied as shown in Fig. 10(a) on a once per tooth basis. For the tests of the study described herein, the measurement location was approximately 1/3 of the distance from the heel to the toe. Shown in Fig. 10(b) are actual infrared microscope and proximity probe outputs taken from a digital storage oscilloscope. As mentioned earlier the proximity probe was used to establish a reference location of the infrared microscope output with respect to a location on the pinion tooth profile.

Also this instrumentation requires a clear line-of-sight, therefore this measurement was made at a rotational distance of approximately 120° out-of-mesh. All infrared microscope signals had a repetitive form similar to that shown in Fig. 10(b) with the voltage differential dependent on the loading conditions that were applied. The calculations made on the raw data are explained in detail in Ref. 9. From the transient infrared oscilloscope data, the tooth tip always produced the highest voltage and the tooth root region the lowest as shown in Fig. 10(b). The sharp decrease in the infrared output (Fig. 10(b)) at points 1,7 and 2 are believed to be due to the pinion top land edge passing in front of the measurement location.

The results found via the infrared microscope will now be discussed. First the variation of speed and load are shown in

Table 3. The thermocouple at the root region was used as the reference temperature to make the calculation from the infrared microscope raw data to the values shown. The temperature difference via the infrared microscope compared fairly well to the temperature differential found via the root and tooth top thermocouples. At the conditions tested speed and load had little effect on the measured values until the full load condition was applied at full speed.

The other set of infrared microscope results to be discussed involved the effect of flow (pressure) and lubricating jet position (Table 4). The infrared microscope data was treated as mentioned above. All the tests were conducted at full load and speed. The infrared microscope produced the same trends as the thermocouples. Lubricating the gear 90° out-of-mesh produced higher pinion operating temperatures than did lubricating the gear 90° before mesh. The infrared microscope temperature differential data when compared to the thermocouples were at the most 11 °C (20 °F) different.

Analytical Model Development:

The spiral bevel gear geometry to be modelled in this study is the face-milled type. This type of system is used for most spiral bevel and hypoid gear meshes manufactured in the United States at this time. A more indepth explanation of the geometry and operation of spiral bevel gears can be found in Refs. 14-22. In this section a brief overview of how a finite element analysis was conducted on the same gear system tested in the prior section will now be made.

Determination of Surface Coordinates: The development of a finite element model for any gear system requires the knowledge of the surface boundaries. The case of face-milled spiral bevel gears requires a kinematic description of the manufacturing process. The process begins by examining the machine tool used in manufacture shown in Fig. 11.

The gear manufacturing machine depicted in Fig. 11 will be used to describe the most important features. First the head cutter, which contains the cutting blades or a grinding wheel, has conical cutting surfaces. The head cutter rotates about it's axis to remove material in the most efficient manner and it's speed is not related to the gear geometry produced. The head cutter orbits about the machine center at a predetermined distance. This location and orientation are dependent on the workpiece basic design data and cutter size. The head cutter and workpiece are respectively rotated about the cradle and axis of rotation of the workpiece in a timed relationship known as the ratio of roll. Typically in aerospace applications the pinion is cut (ground) one side of the tooth profile at a time whereas the gear is simultaneously cut (ground) on both sides. Therefore many machine settings will differ from one side to the other for the pinion.

From the differential geometry approach of Ref. 16, a description of the relationship between the head cutter and the workpiece can be found and is called the "equation of meshing." For the profile coordinates of a spiral bevel gear three unknown parameters from the differential geometry description along with the basic machine settings and gear design data are combined to produce a system of three nonlinear algebraic equations that are solved numerically. Once these coordinates are found for the pinion or gear under study, a finite element model can be produced as shown in Fig. 12.

Tooth Contact Analysis, Three-Dimensional Contact, Heat Generation, and Heat Transfer Coefficients:

The next part of the analysis to be described is how the finite element model boundary conditions are determined and applied. The boundary conditions are found using a three step approach. First tooth contact analysis from the gear tooth surface geometry is needed to describe the interacting surfaces. Secondly a three-dimensional Hertzian contact analysis on the geometry of the contacting points is conducted. Based on the tooth contact and Hertzian analysis the frictional heat generation can be determined. Finally the heat transfer coefficients are determined from empirical results where possible.

Tooth Contact Analysis: First the tooth contact analysis described in Ref. 16 is used. The machine tool settings and gear mesh operating conditions are used as input to this analysis. Based on the input provided the program determines the unloaded transmission error as a function of roll angle, location of the instantaneous point of contact, the principal curvatures and orientations, the sliding and rolling velocity, and the normal force assuming a single pair of teeth are in contact.

The transmission error as a function of roll angle is used to determine the level of load that is to be applied at any point of contact. Where there is an overlap of the parabolic transmission error curves the load is assumed to be equally shared between two pairs of teeth [9-10].

Three-Dimensional Contact: The other geometrical properties of the contacting points are used in a three-dimensional contact analysis [23,24]. From the principal curvatures, orientations, material properties, and load the contact region is determined. The contact region for any particular ellipse is the found on the finite element model by determining which surface grid points from the tooth profile are contained within the ellipse [9].

Heat Generation: In this study only the heat generated due to the relative sliding of the meshing teeth is assumed to exist. The heat flux can be described as the product of the friction coefficient, sliding velocity, and load. The friction coefficient as a function of rolling velocity, sliding velocity, oil inlet temperature, and maximum contact pressure was described for a turbine engine oil in Refs. 9, 25. The sliding and rolling velocity are found using tooth contact analysis, the inlet lubricant temperature is known, and the maximum contact pressure is determined by the three-dimensional contact analysis. Therefore the heat flux as a function of contact location for the model is now available.

Heat Transfer Coefficients: The last boundary conditions necessary for a thermal analysis are the heat transfer coefficients for the pinion under consideration. In the study conducted herein a one-tooth sector model was used (Fig. 12). Where the model was cut between adjacent teeth the boundary was assumed to be insulated or no heat transfer takes place. On the other exposed surfaces the heat transfer forced convection boundaries were treated as flat plates, or rotating disks, or the coefficients were estimated where no empirical data was applicable.

Analytical Results:

Based on the methods mentioned previously, a thermal finite element analysis of an in-house test specimen was developed [10]. The model developed is that shown in Fig. 12. This model has 20 250 elements, and 22 586 grid points, with 874 of these grid points on the active profile. The geometric model was created using the program developed in Ref. 18 that outputs a file that can be directly read into a geometric modelling package [26]. The finite element model used the full load and speed conditions as shown in Table 1. Fifteen contact (ellipse) locations over the entire meshing cycle for one pair of teeth were used. The sliding velocity based on these conditions and the lubricant friction coefficient as a function of meshing location are shown in Fig. 13. The load applied at each of the contact locations, based on the load sharing already mentioned, and the resultant heat flux are also shown as a function of meshing location in Fig. 14. The maximum heat flux for this model occurs at the highest point of single tooth pair contact.

During meshing for this model (pinion), the grid points exposed to the heat flux on the active profile change for each meshing position. Figure 15 shows an example of one of the meshing locations (number 9 of 15 total). The entire active profile is projected on an axial-radial plane. The filled circles are the ones that have heat flux applied for this meshing location. The composite of all meshing positions for all ellipses would predict the contact pattern for the loaded gear system. Therefore the heat flux locations with respect to meshing position are very important to the time- and position-varying boundary conditions that need to be established.

The nonlinear finite element code used for the analysis [27] permits time- and position-varying boundary conditions to be applied through the use of "user subroutines." User subroutines were written for a time averaged set of boundary conditions and for a time- and position-varying boundary conditions. Time averaging of the boundary conditions were needed to move the analysis out to a point in time where the overall model behaves in a thermal equilibrium state. This is very useful for models that have very small time step increments in the transient mode and would required millions of time steps to reach steady state. Using the time averaged boundary conditions to move out in elapsed time and then switching user subroutines to the time- and position-varying conditions saves a monumental amount of super computer CPU time.

This procedure was implemented for this study. Figure 16 shows the temperature history after changing from the time-averaged to the time- and position-varying boundary conditions for a grid point on the active profile. Each time the heat flux passes over the grid point, a temperature change of approximately 37 °C (67 °F) occurs. This flash of temperature is then followed by the forced convection cooling that follows until the next meshing period. Note that in Fig. 16 that the time-varying temperature is very repeatable even after just a couple of revolutions. An example of the full three-dimensional temperature field is shown in Fig. 17. This particular figure is from heat flux ellipse #13. The maximum temperature predicted at this point during the meshing process is 200 °C (392 °F).

At locations away from the active profile no change in temperature is indicated when changing from the time averaged to transient boundary conditions. Only locations in close proximity to the moving heat flux are affected during the transient operation.

Comparison of Experiments and Analysis:

A comparison of the experimental and analytical results will now be made. The data taken via thermocouples will be compared with the same locations on the finite element model. The infrared microscope data will be compared to the results from the transient model at the same out-of-mesh location where the data was taken.

The comparison between the thermocouples and the analysis is shown in Fig. 18. Two experimentally different lubrication effects were compared to the steady state results of the analysis with some minor changes to the heat transfer coefficients and ambient conditions. As shown in the figure, the analysis did bracket the temperature found at the four locations. As mentioned earlier, available heat transfer coefficients for gears are nonexistent and the assumed ambient conditions could be adjusted to duplicate the results found through experiments. Fine tuning of the model via the boundary conditions could be utilized to develop a range of heat transfer coefficients based on flow rate, lubricant jet location, rotational speed, and other effects.

The other comparison to be made is that of the infrared microscope and the transient numerical finite element solution. In Fig. 19 the path of the infrared microscope superimposed on the thermal model at the 120° out-of-mesh position is shown. Note that due to alignment of the infrared microscope the hottest locations of the active profile of the pinion were not traversed. The resultant transient measurement and analytical result are shown in Fig. 20. The transient analytical solution was fixed at one location at the 120° out-of-mesh position. The model could have been checked at each time step increment during the period of time it takes the infrared microscope to traverse one tooth cycle. The model showed a temperature variation of approximately 30 °C (54 °F) at the region that the infrared microscope traversed.

The infrared microscope data shown in Fig. 20 will be further explained. The infrared microscope in the transient mode requires a reference temperature to perform the calculations on the raw data gathered during the experiment. Since a direct comparison to the analysis was to be made, the analytical prediction for the region at the root where the infrared microscope traversed the root (start of active profile) was used as the reference temperature. The only other effect factored into the calculation of temperature differential from the raw data was the attenuating effect of the lens system between the infrared microscope and the test specimen as explained in Ref. 9. Other effects on the raw data such as orientation of the infrared microscope with respect to the surface and gear edge effects were not considered. Therefore a minimum of special treatment to the raw data was used for the comparison shown in Fig. 20. The analytical and experimental results showed similar trends except at the location where the pinion active profile and tooth top corner is traversed. The rest of the results were within 10 percent of each other at the other locations.

Conclusions:

An experimental and analytical study have been conducted with respect to the thermal behavior of spiral bevel gears. The experimental effort was conducted on aerospace quality spiral bevel gears at rotational speeds to 14 400 rpm and 537 kW (720 hp). The experimental results indicated that load, jet location, flow rate, and oil inlet temperature all can affect the steady state operating tem-

perature of the spiral bevel pinions that were instrumented. Also an analytical modelling method was developed to analyze the thermal behavior via the finite element method.

Based on the study conducted the following conclusions can be drawn:

(1) The experimental study found that: (i) Bulk temperatures varied nearly linearly with increasing load and oil inlet temperature; (ii) Lubricant jet placement at either the into- or out-of-mesh positions produced the lowest operating temperatures; and (iii) Infrared measurements indicated that there are substantial temperature differences across the active profile, and at the location where the instrument measured the transient temperature the tooth top was the highest temperature which is the same pattern found in the thermocouple measured data.

(2) A finite element based, three-dimensional, thermal analysis of spiral bevel gears was developed. The model predicts the entire temperature distribution of the spiral bevel gear. From this model regions located a distance from the active profile do not experience rapid transient temperature changes as was found on the active profile (up to 37 °C). These regions stay essentially at their final steady state solution temperature throughout the once per revolution heat flux/ convection cooling cycle.

(3) Comparisons between the experimental and analytical results generally were in agreement. At locations where bulk temperature (steady state) measurements using thermocouples were made the results found analytically bracketed the experimental results. Across the active profile where the heat flux is imparted to the test hardware and analytical model, the trends agreed between an infrared microscope and the time varying transient solution at the measurement location of approximately 120° after meshing had occurred.

References:

[1] Lewicki, D. and Coy, J.: "Vibration Characteristics of OH–58A Helicopter Main Rotor Transmission," NASA TP–2705, AVSCOM TR 86–C–42, April, 1987.

[2] Borsoff, V.: "Predicting the Scoring of Gears," Machine Design, Vol. 37, Jan., 1965.

[3] Townsend, D.: "Lubrication Considerations in Gear Design," NASA TM X–52942, Dec. 1970.

[4] Blok, H.: "Theoretical Study of Temperature Rise at Surface of Actual Contact Under Oiliness Lubricating Conditions," I. Mech. E., London, Proc. Gen. Disc. Lubrication, Vol. 2, 1937.

[5] Blok, H.: "Measurement of Temperature Flashes on Gear Teeth Under Extreme Pressure Conditions," I. Mech. E., London, Proc. Vol. 1–2, 1937.

[6] Coleman, W.: "A Scoring Formula for Bevel and Hypoid Gear Teeth," J. of Lubrication Technology, Trans. of the ASME, April, 1967.

[7] "Scoring Resistance of Bevel Gear Teeth," The Gleason Works, Rochester, New York, 1966.

[8] Chao, H., and Cheng, H.: "A Computer Solution for the Dynamic Load, Lubricant Film Thickness, and Surface Temperatures in Spiral Bevel Gears," NASA CR–4077, July, 1987.

[9] Handschuh, R.: "Thermal Behavior of Spiral Bevel Gears," Ph.D. Dissertation, Case Western Reserve University, August, 1993.

[10] Handschuh, R., and Kicher, T.: "A Method for Thermal Analysis of Spiral Bevel Gears," NASA TM–106612, ARL–TR–457, September, 1994.

[11] Wyner, D.; and Macpherson, P.: An Infra-Red Technique for Monitoring Gear Tooth Surface Temperatures. Research Paper RP 458, Contract No. K 25B/534/cb25B, Imperial College, London, England, Jan. 1974.

[12] Ku, P; Staph, H.; and Carper, H.: Gear Tooth Scoring Investigation. Report USAAMRDL–TR–75–33, Southwest Research Institute, San Antonio, TX, July 1975.

[13] Handschuh, R.: Effect of Lubricant Location on Spiral Bevel Gear Operating Temperatures. NASA TM–105656, 1992.

[14] Litvin, F.: Theory of Gearing, NASA RP–1212, AVSCOM TR–88–C–035, Dec. 1989.

[15] Litvin, F., and Lee, H.: "Generation and Tooth Contact Analysis of Spiral Bevel Gears With Predesigned Parabolic Functions of Transmission Errors," NASA CR–4259, AVSCOM TR 89–C–014, 1989.

[16] Litvin, F., and Zhang, Y.: "Local Synthesis and Tooth Contact Analysis of Face-Milled Spiral Bevel Gears," NASA CR–4342, AVSCOM TR–90–C–028, 1991.

[17] Litvin, F., Zhang, Y., and Handschuh, R.: "Local Synthesis and Tooth Contact Analysis of Face-Milled Spiral Bevel Gears," NASA TM–105182, AVSCOM TR 91–C–039, Sept. 1991.

[18] Handschuh, R., and Litvin, F.: "A Method for Determining Spiral Bevel Gear Tooth Geometry for Finite Element Analysis," NASA TP–3096, AVSCOM TR–91–C–020, Aug., 1991.

[19] Fong, Z., and Tsay, C.: "A Mathematical Model for the Tooth Geometry of Circular-Cut Spiral Bevel Gears," J. of Mech. Design, Vol. 113, June 1991.

[20] "Understanding Tooth Contact Analysis," The Gleason Works, Rochester, New York, 1981.

[21] Gosselin, C., Cloutier, L., and Brousscue, J.: "Tooth Contact Analysis of High Conformity Spiral Bevel Gears," JSME Int. Conf. on Motion and Power Transmission, Hiroshima, Japan, Nov. 1991.

[22] Gosselin, C., Cloutier, L., and Nguyen, Q.: "The Influence of the Kinematical Motion Error of Spiral Bevel Gears," AGMA Fall Technical Meeting, 1992.

[23] Timoshenko, S., and Goodier, J.: Theory of Elasticity, McGraw-Hill, 1951.

[24] Boresi, A., Sidebottom, O., Seely, F., and Smith, J.: Advanced Mechanics of Materials, John Wiley & Sons, 1978.

[25] Tevaarwerk, J.: "Constitutive Modeling of Lubricants in Concentrated Contacts at High Slide to Roll Ratios," NASA CR–175029, Dec. 1985.

[26] PDA Engineering, PATRAN Plus, Release 2.5, Costa Mesa, CA, 1991.

[27] MARC Finite Element Program, Revision K4-1, Marc Analysis Research Corporation, Palo Alto, CA, 1990.

TABLE 1.—SPIRAL BEVEL GEAR TEST FACILITY PARAMETERS AT FULL SPEED AND LOAD CONDITIONS

Pinion shaft speed, rpm	14 400
Pitch line velocity, m/s (ft/min)	44.7 (8803)
Pinion shaft power, kW (hp)	537 (720)
Test section flow rate maximum, cm3/s (gal/min)	51 (0.8)
Oil inlet temperature (variable), °C (°F)	38 to 189 (100 to 300)
Oil pressure maximum, MPa (psi)	1.38 (200)

TABLE 2.—TEST SPECIMEN DESIGN PARAMETERS

Number of teeth pinion/gear	12/36
Diametral pitch	5.141
Mean spiral angle, deg	35
Mean cone distance, mm (in.)	81.1 (3.191)
Face width, mm (in.)	25.4 (1.0)
Nominal pressure angle, deg	22.5
Shaft angle, deg	90
AGMA class	12
AGMA bending stress index, MPa (ksi)	398 (57.7)
AGMA contact stress index, MPa (ksi)	2406 (349)

TABLE 3.—CALCULATED INFRARED TEMPERATURE DIFFERENCE FOR FOUR OPERATING CONDITIONS COMPARED TO THERMOCOUPLES

[Pencil jet 0.51 mm (0.02 in.) diameter, oil inlet pressure 1.38 MPa (200 psi), oil inlet temperature 57 °C (135 °F), and jet positioned on gear 90° into mesh on the gear.]

Pinion operating conditions			Thermocouple location				Temperature difference			
Speed, rpm	Torque		Root		Top		Thermocouple (top-root)		Infrared microscope	
	N*m	in.*lb	°C	°F	°C	°F	°C	°F	°C	°F
7 200	177	1567	75	167	103	217	28	50	29	52
10 800	267	2363	118	244	146	295	28	51	30	54
14 400	267	2363	136	277	166	331	30	54	30	54
14 400	354	3133	154	309	188	370	34	61	40	72

TABLE 4.—COMPARISON OF THERMOCOUPLE AND INFRARED MICROSCOPE MAXIMUM TEMPEATURE DIFFERENCE FOR TWO LUBRICANT JET POSITIONS AND TWO JET PRESSURES

[Pinion speed = 14 400 rpm; pinion torque = 354 N*m (3 133 in.*lb), oil inlet temperature = 38 °C (100 °F).]

Jet location on gear[a]	Lubricant fan jet		Thermocouple location				Temperature difference			
	Pressure	Flow	Root		Top		Thermocouple (top-root)		Infrared microscope	
	MPa (psi)	cm^3/sec (gpm)	°C	°F	°C	°F	°C	°F	°C	°F
A	1.38 (200)	49 (0.78)	124	255	164	327	40	72	29	52
A	0.35 (51)	25 (0.40)	134	273	175	347	41	74	32	58
B	1.40 (203)	49 (0.78)	123	253	154	309	31	56	26	47
B	0.35 (51)	25 (0.40)	127	261	161	322	34	61	28	50

[a]A = 90° out-of-mesh on the gear.
B = 90° before mesh on the gear.

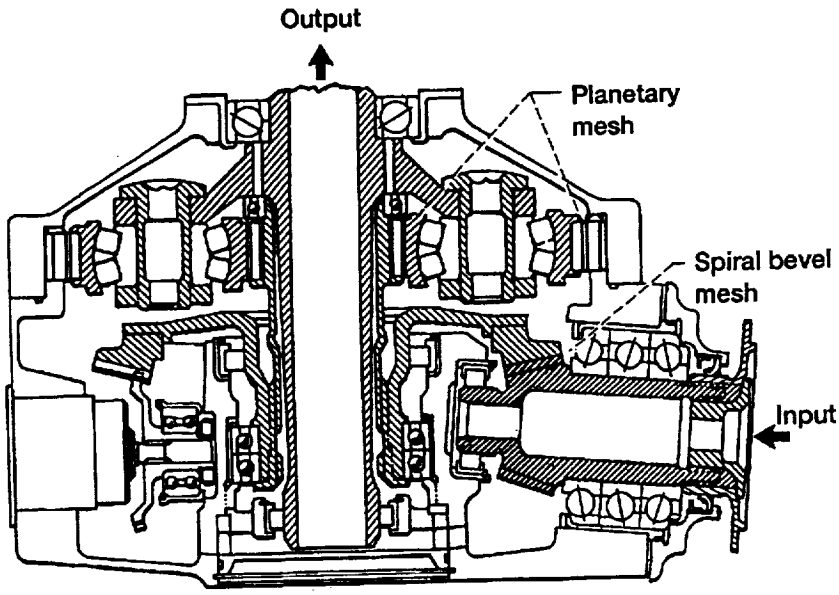

Figure 1.—OH-58A helicopter main rotor transmission. (Ref. [1]).

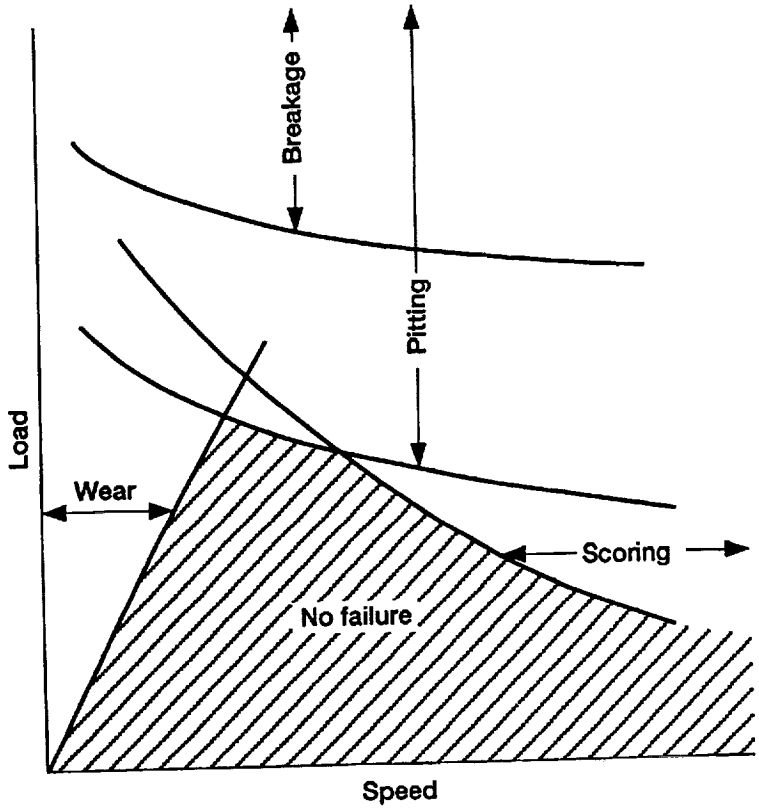

Figure 2.—Gear design parameters of concern based on operating conditions (Ref. [2,3]).

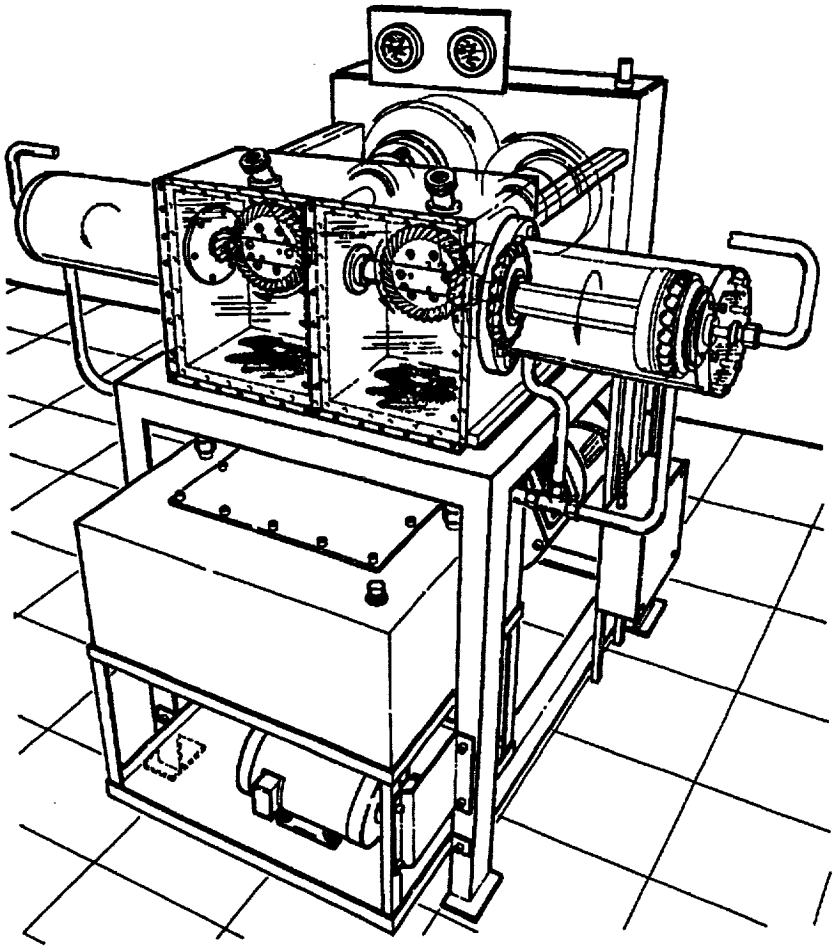

Figure 3.—Spiral bevel test facility sketch.

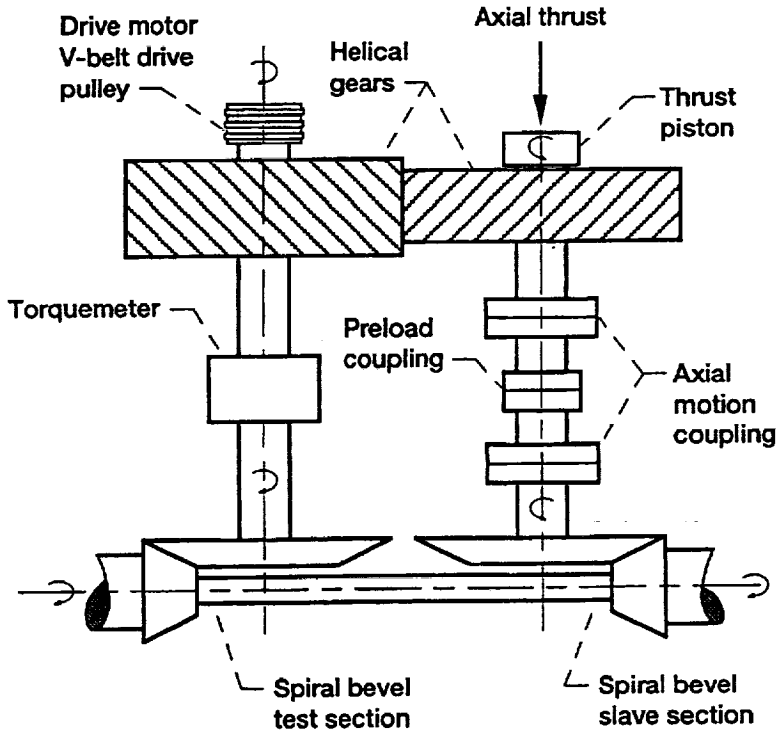

Figure 4.—Cross-sectional view of spiral bevel test facility.

Figure 5.—Bulk thermocouple pinion.

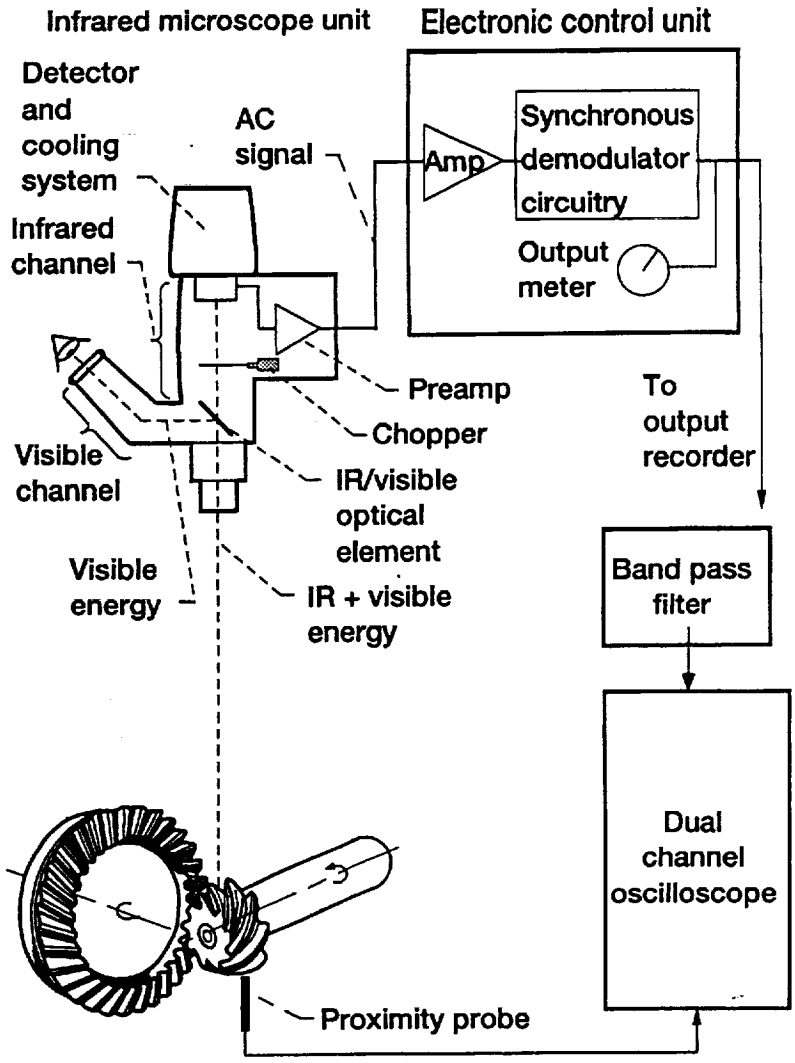

Figure 6.—Transient temperature measurement system.

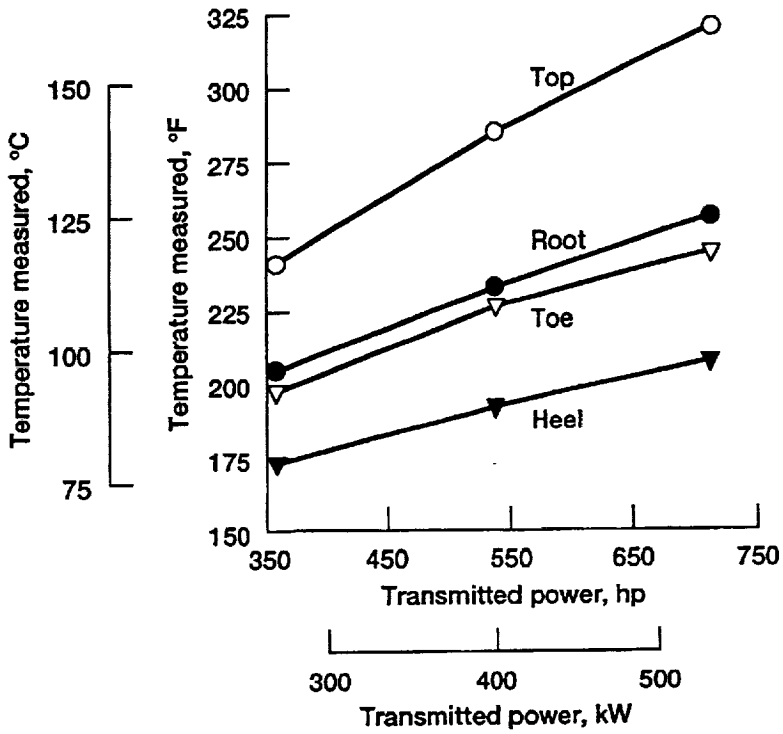

Figure 7.—Effect of load on pinion tooth temperatures at three power levels. All data taken at 38 °C (100 °F) oil inlet temperature and 14 400 rpm pinion shaft speed.

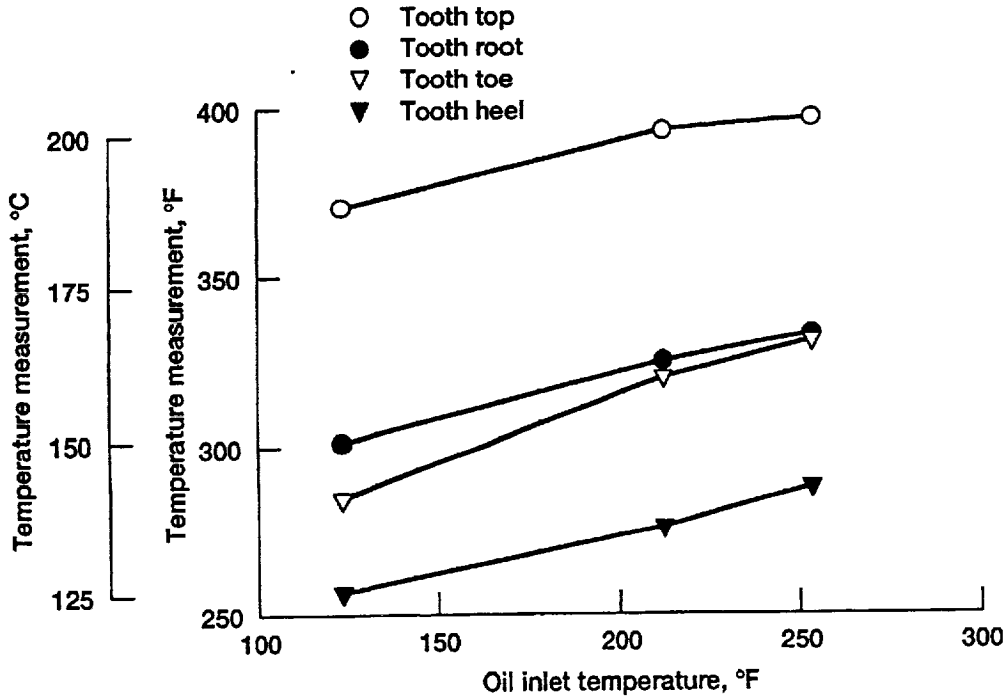

Figure 8.—Effect of oil inlet temperature on pinion temperature. Pencil jet oriented on the gear 90° before mesh. Oil jet pressure, speed, load held constant at 0.34 MPa, 14 400 rpm, 359 N•m (3130 in.•lb) respectively.

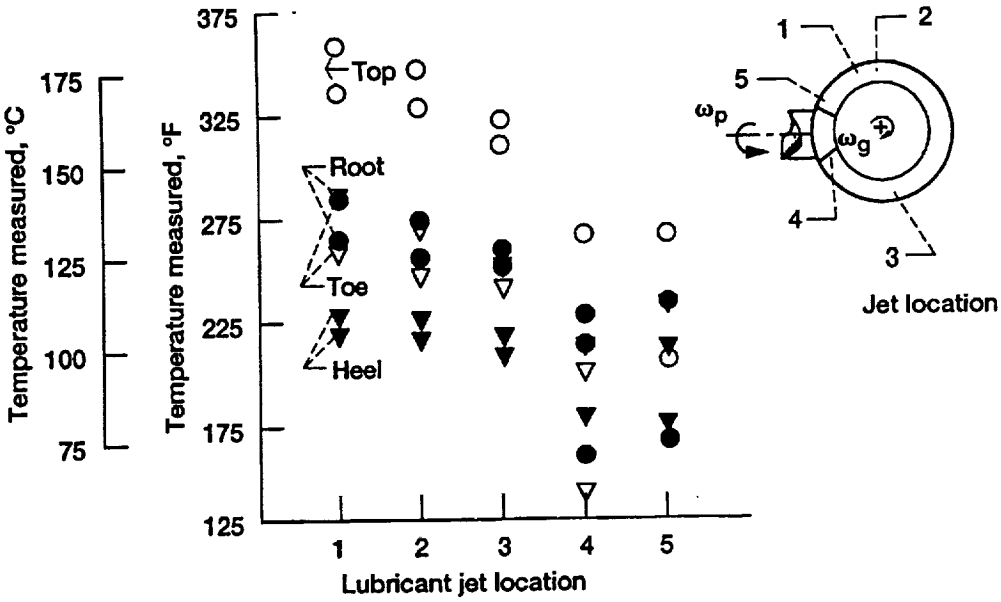

Figure 9.—Effect of lubricant jet location on pinion thermocouple measurements for two flow rates at 526-538 kW (705-721 hp). Upper symbol is for 24 cm^3/sec (0.38 gpm) and lower symbol is for 49 cm^3/sec (0.77 gpm).

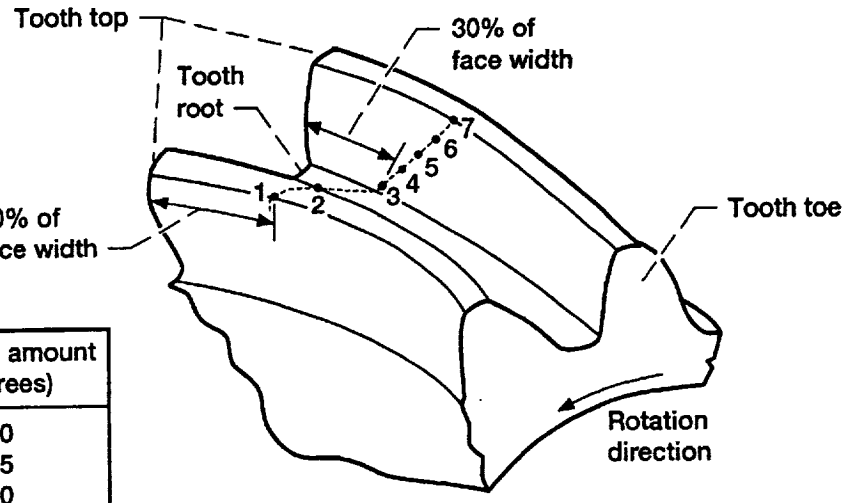

Position of measurement	Rotation amount (degrees)
1	0
2	5
3	10
4	15
5	20
6	25
7	30

(a) Infrared measurement path.

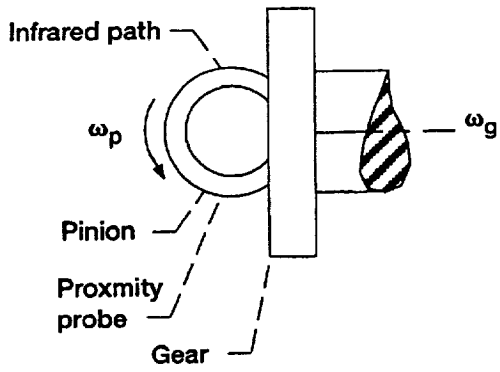

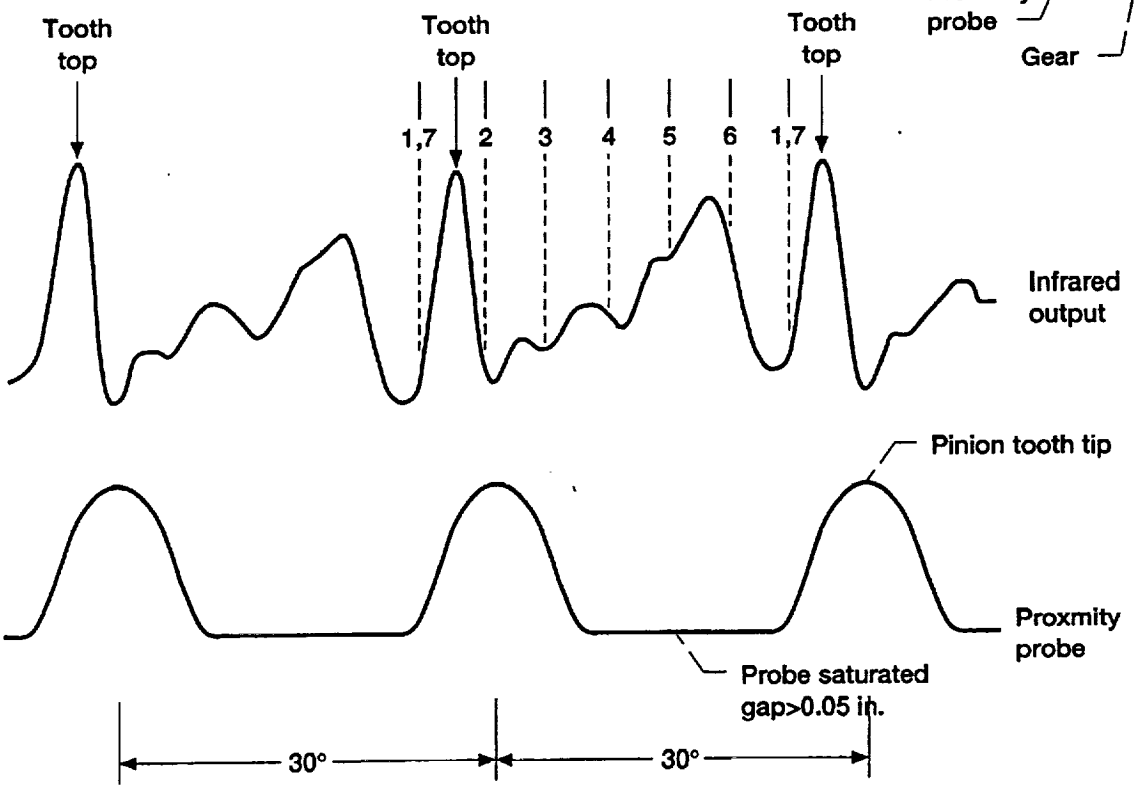

(b) Infrared path located on infrared output.

Figure 10.—Infrared path with respect to an infrared output measurement.

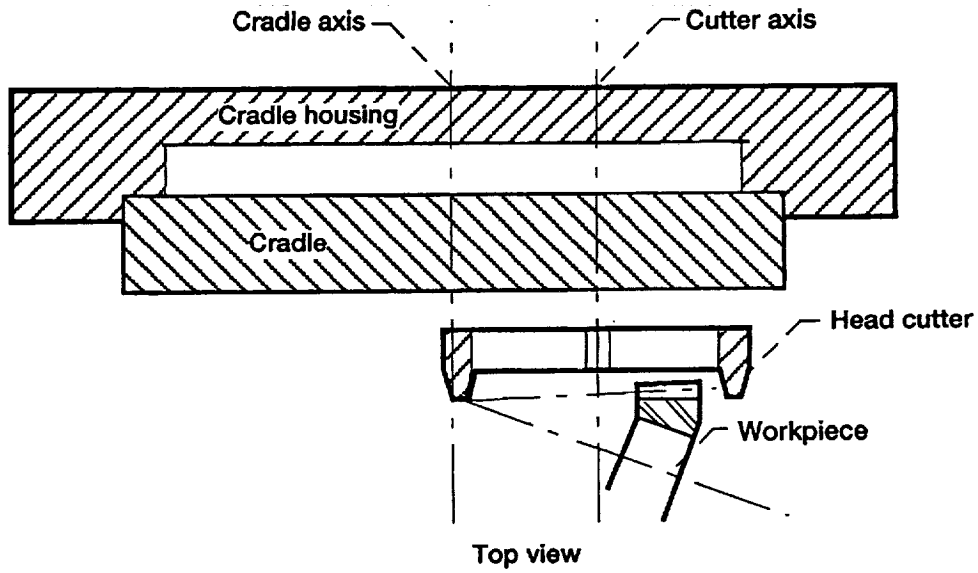

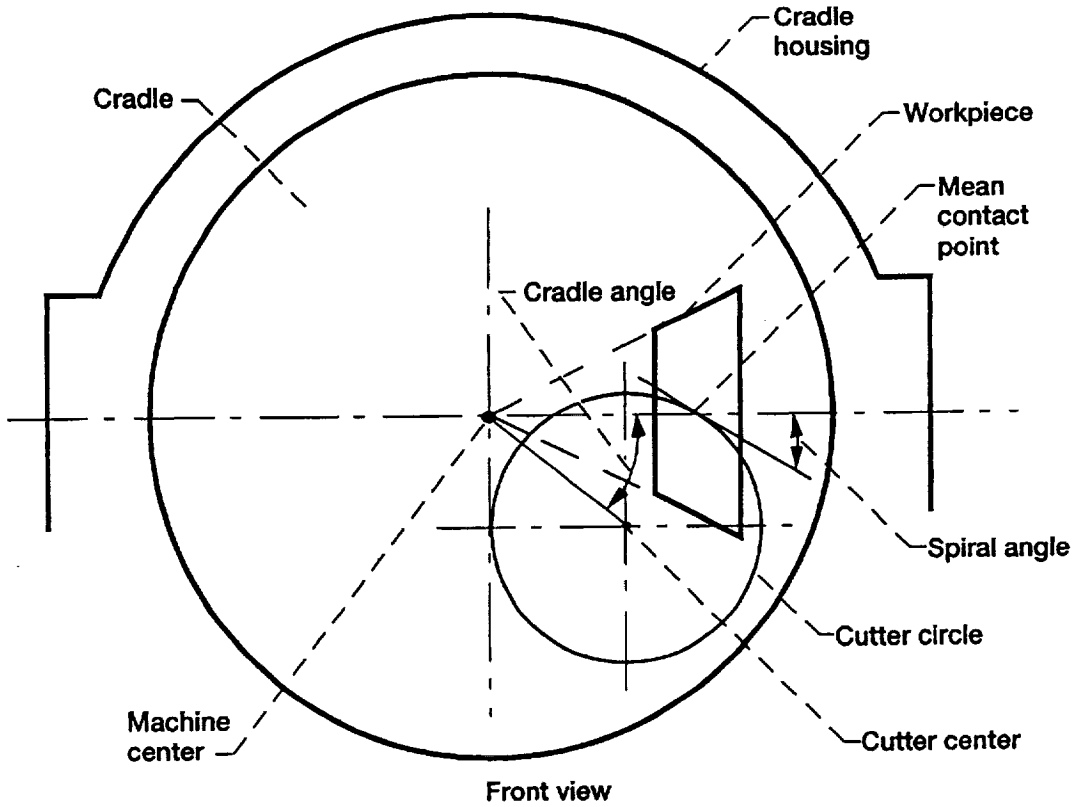

Figure 11—Orientation of workpiece to generation machinery.

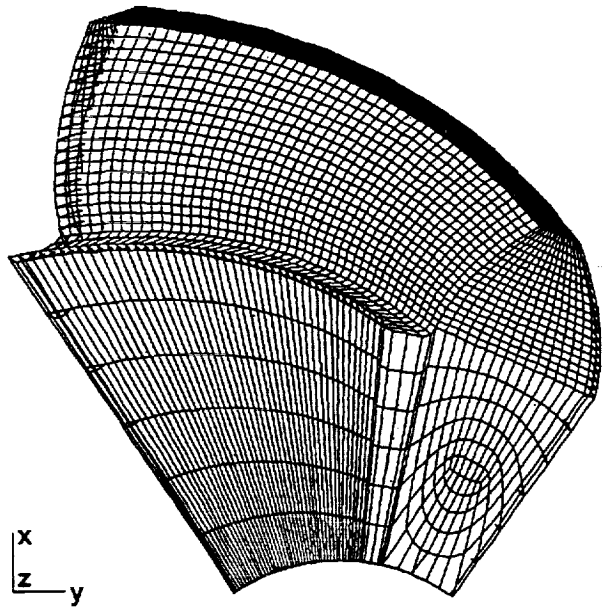

Figure 12.—Finite element model used for heat transfer study.

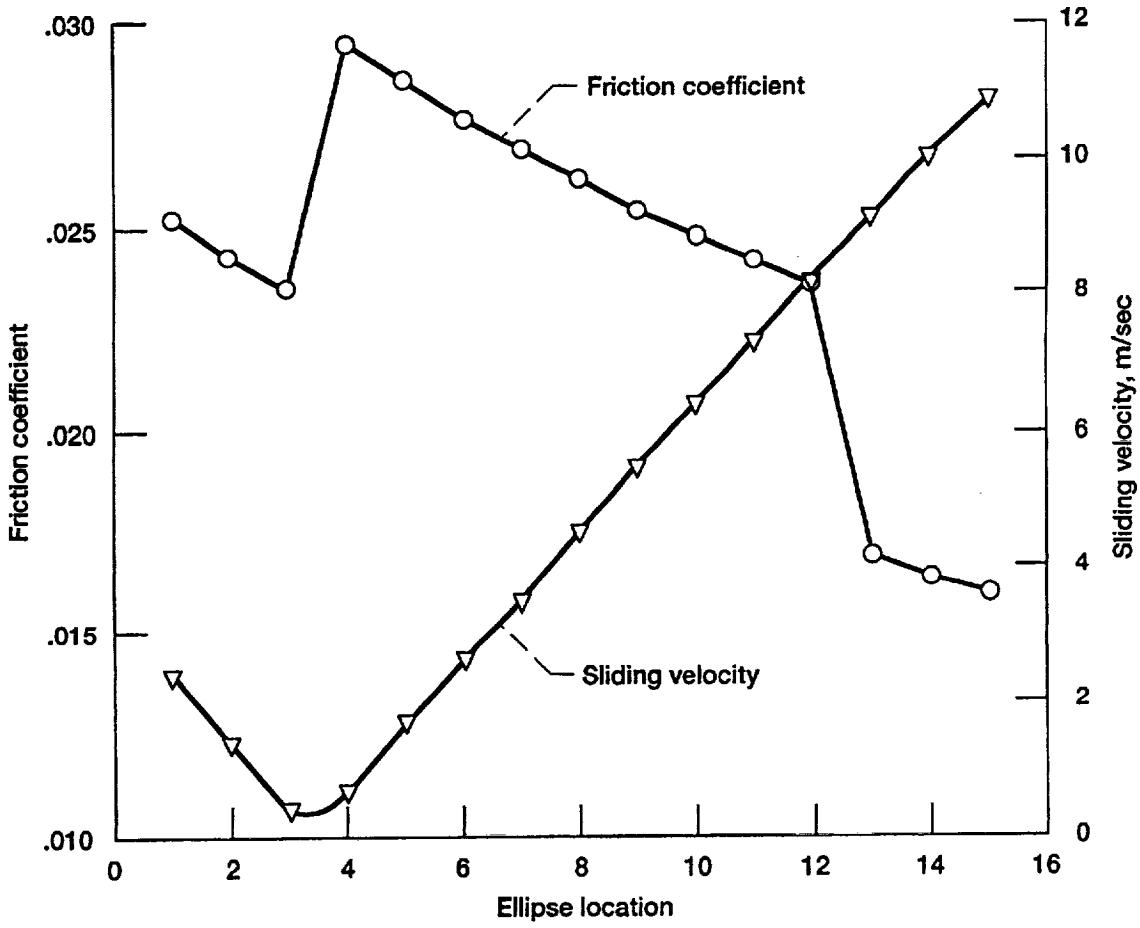

Figure 13.—Friction coefficient and sliding velocity as function of ellipse location.

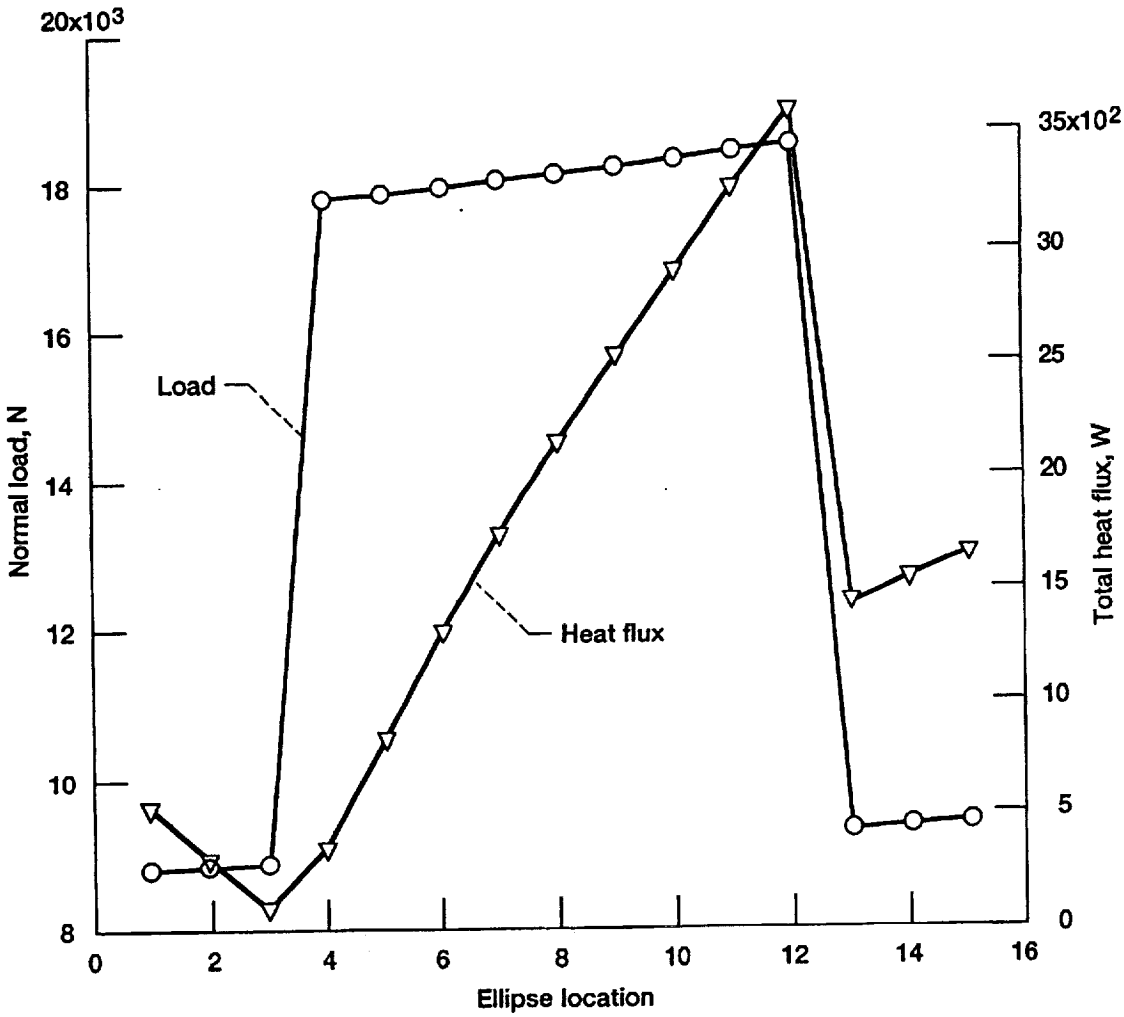

Figure 14.—Load and heat flux as a function of ellipse location.

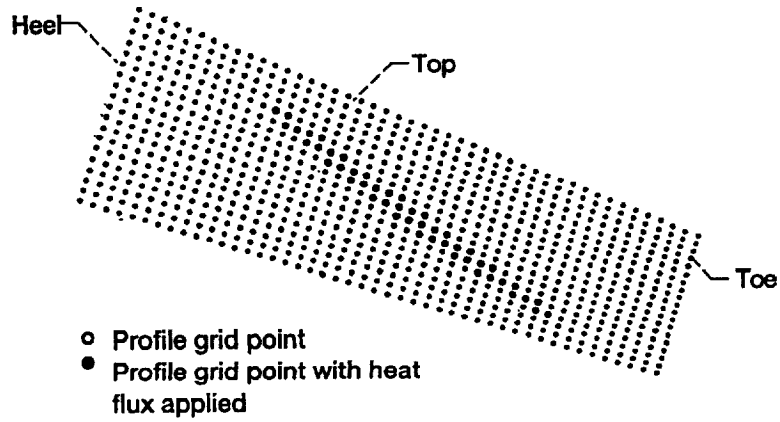

Figure 15.—Contact ellipse number 9 of 15, shown plotted on the entire concave profile grid.

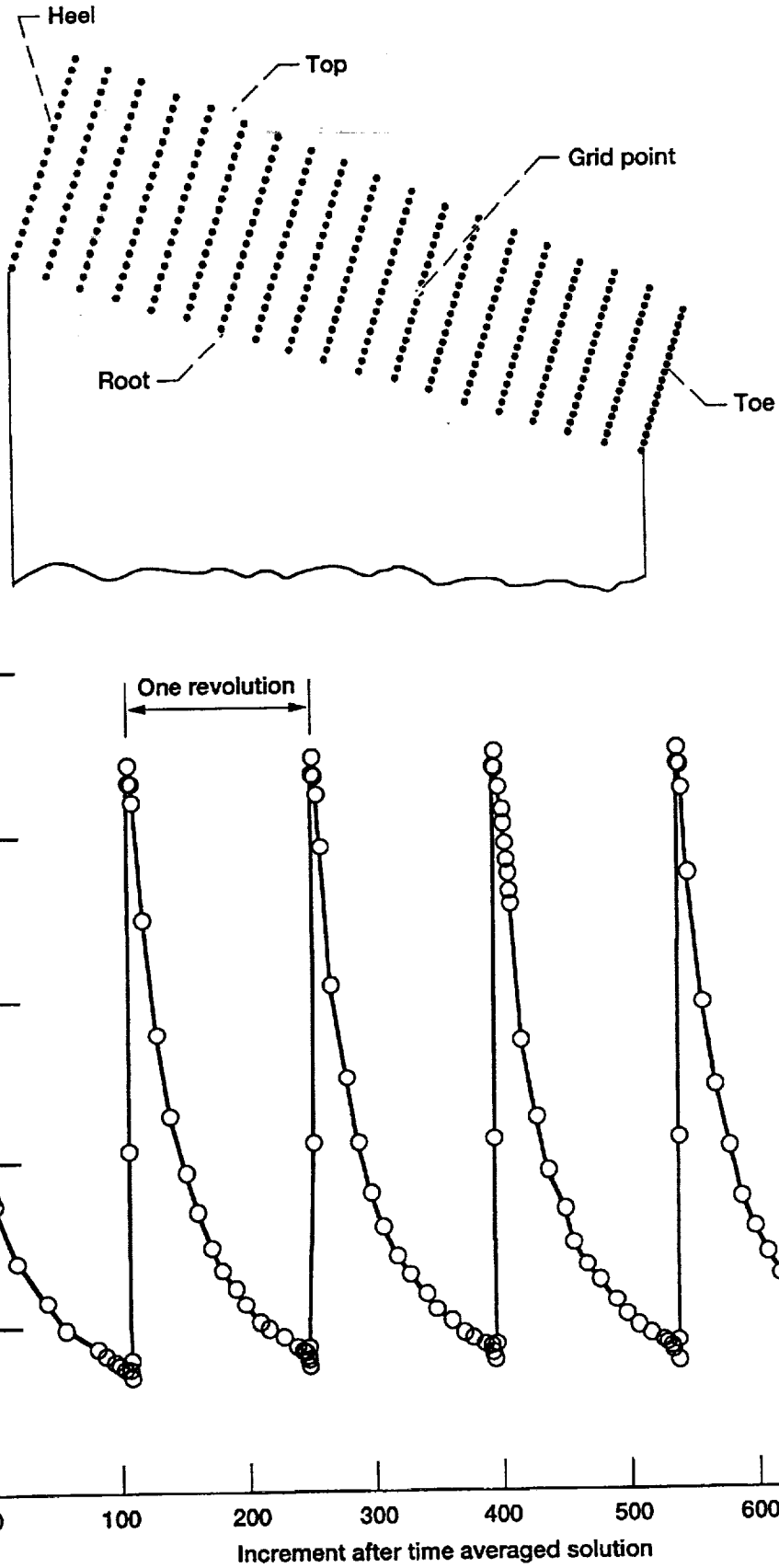

Figure 16.—Active profile grid point location and temperature transient.

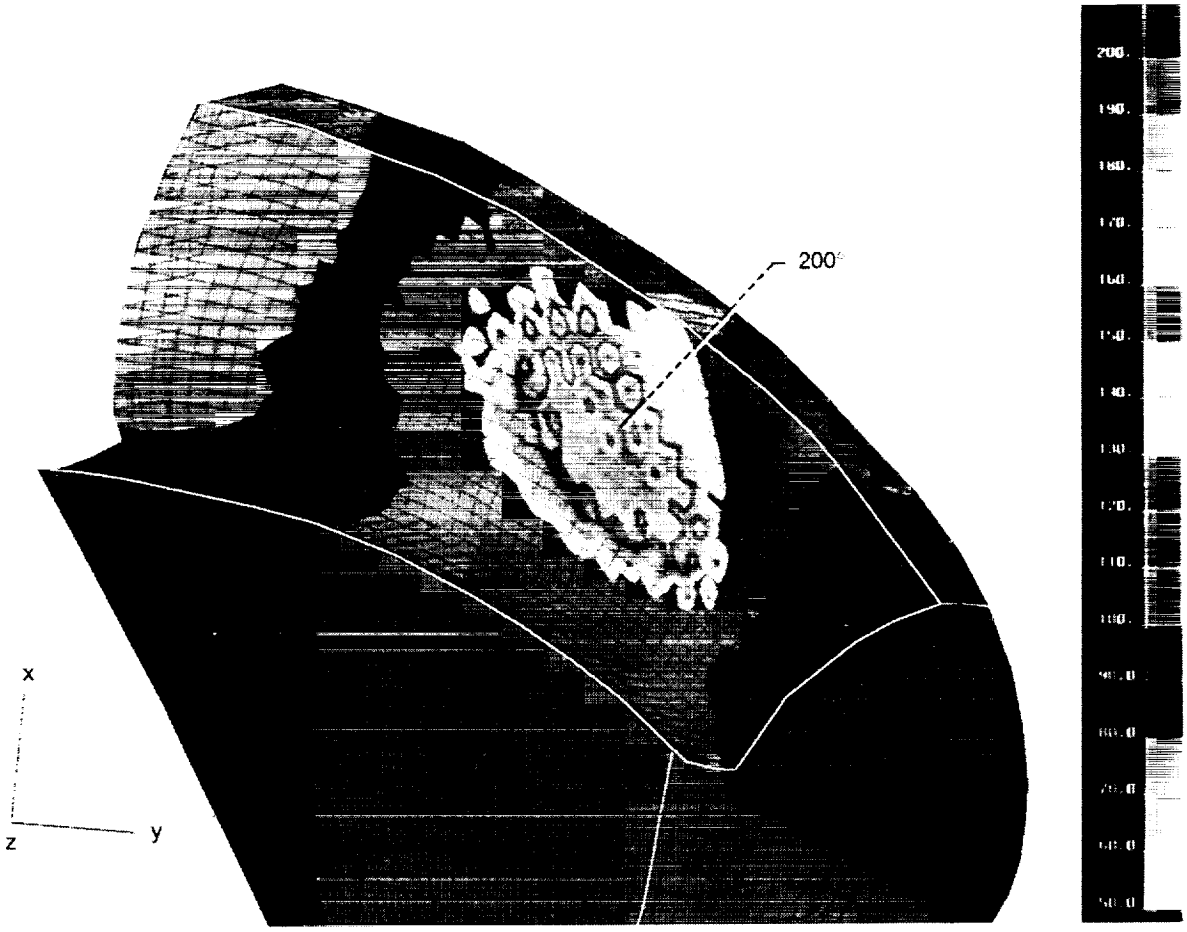

Figure 17.—Heat flux increment 13, temperature °C .

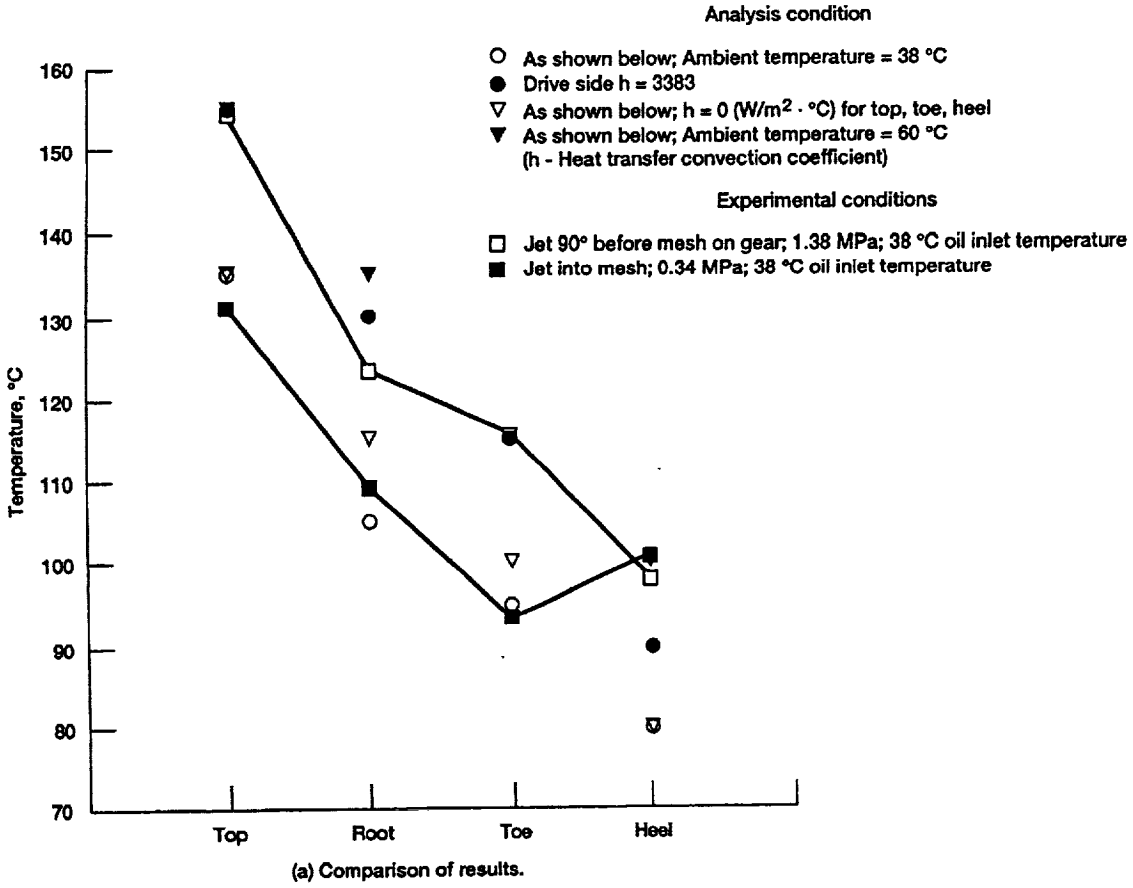

(a) Comparison of results.

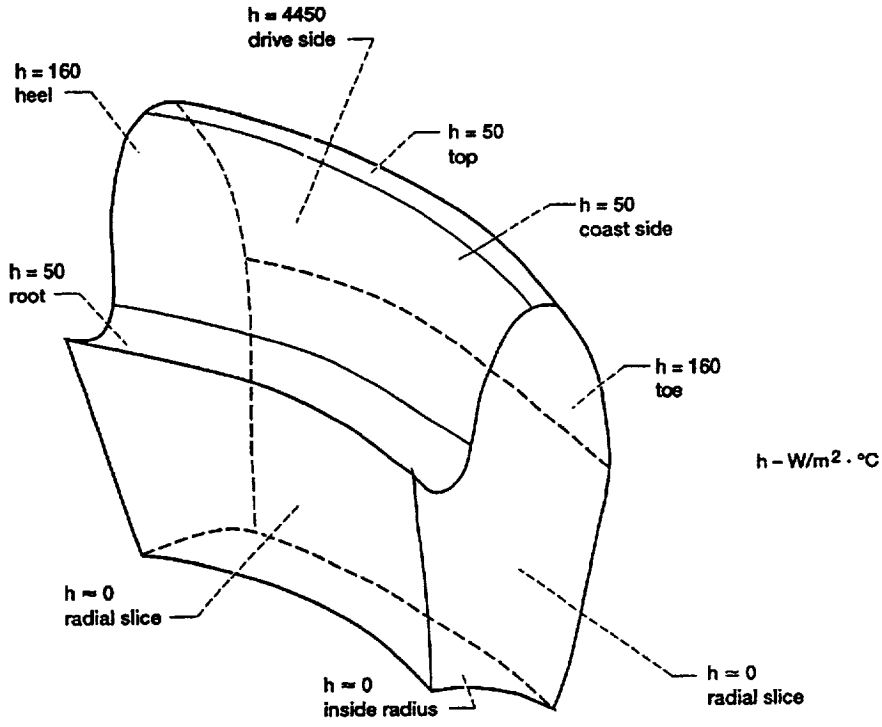

(b) Heat transfer convection coefficients, h.

Figure 18.—Comparison of bulk measurments from thermocouples to time-averaged boundary condition analytical results.

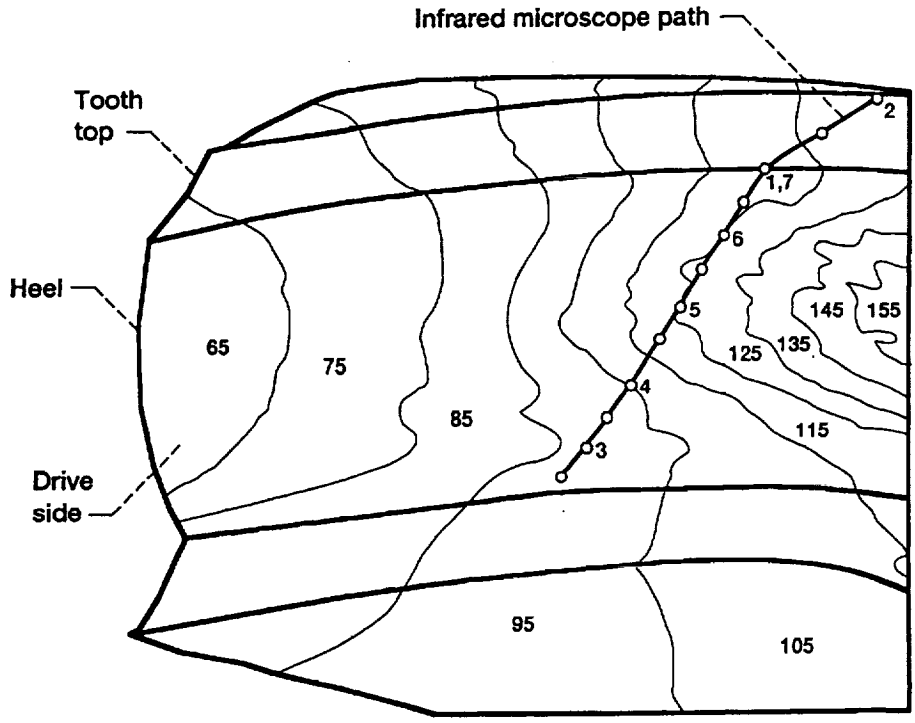

Figure 19.—Temperature field of pinion at 120° out-of-mesh position. Model is shown from approximately half the face width to the heel. Infrared path locations are numbered to relate to Figure 10(b). Temperature shown is in degrees centigrade.

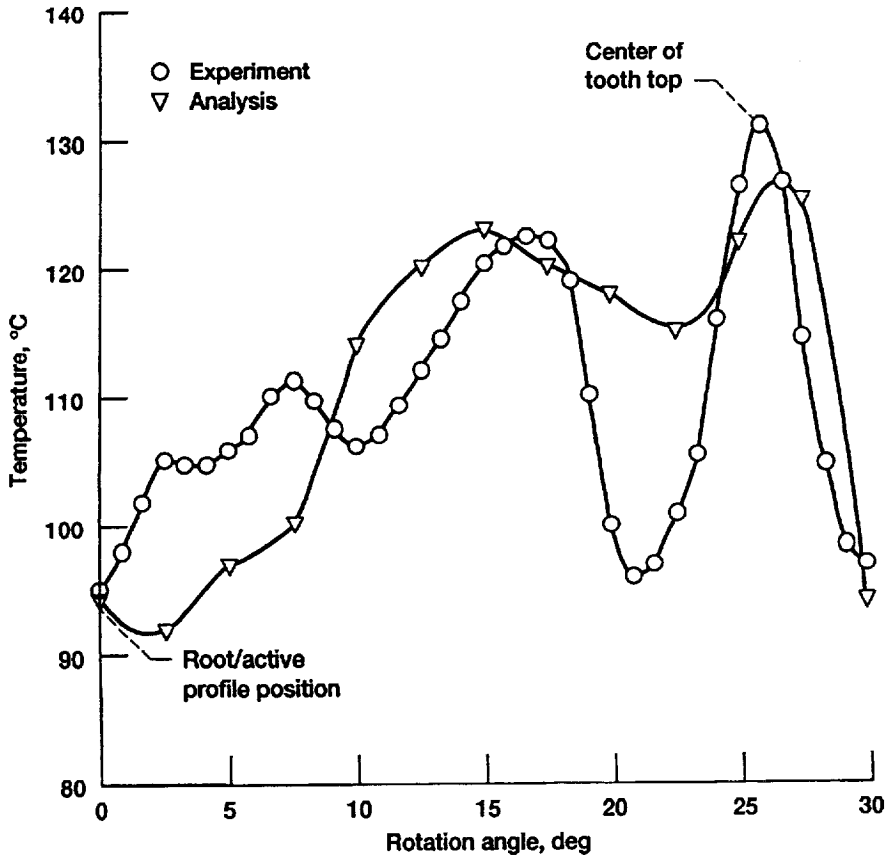

Figure 20.—Comparison of infrared microscope results with that predicted with the analysis that was developed.

REPORT DOCUMENTATION PAGE

Form Approved
OMB No. 0704-0188

1. AGENCY USE ONLY (*Leave blank*)	2. REPORT DATE	3. REPORT TYPE AND DATES COVERED
	August 1995	Technical Memorandum

4. TITLE AND SUBTITLE

Experimental and Analytical Assessment of the Thermal Behavior of Spiral Bevel Gears

5. FUNDING NUMBERS

WU–505–62–36
1L162211A47A

6. AUTHOR(S)

Robert F. Handschuh and Thomas P. Kicher

7. PERFORMING ORGANIZATION NAME(S) AND ADDRESS(ES)

NASA Lewis Research Center
Cleveland, Ohio 44135–3191
and
Vehicle Propulsion Directorate
U.S. Army Research Laboratory
Cleveland, Ohio 44135–3191

8. PERFORMING ORGANIZATION REPORT NUMBER

E–9793

9. SPONSORING/MONITORING AGENCY NAME(S) AND ADDRESS(ES)

National Aeronautics and Space Administration
Washington, D.C. 20546–0001
and
U.S. Army Research Laboratory
Adelphi, Maryland 20783–1145

10. SPONSORING/MONITORING AGENCY REPORT NUMBER

NASA TM–107009
ARL–TR–852

11. SUPPLEMENTARY NOTES

Prepared for the 1995 Fall Technical Meeting sponsored by the American Gear Manufacturers Association, Charleston, South Carolina, October 16–18, 1995. Robert F. Handschuh, Vehicle Propulsion Directorate, U.S. Army Research Laboratory, NASA Lewis Research Center and Thomas P. Kicher, Case Western Reserve University, Cleveland, Ohio 44106. Responsible person, Robert F. Handschuh, organization code 2730, (216) 433–3969.

12a. DISTRIBUTION/AVAILABILITY STATEMENT

Unclassified - Unlimited
Subject Category 37

This publication is available from the NASA Center for Aerospace Information, (301) 621–0390.

12b. DISTRIBUTION CODE

13. ABSTRACT (*Maximum 200 words*)

An experimental and analytical study of spiral bevel gears operating in an aerospace environment has been performed. Tests were conducted within a closed loop test stand at NASA Lewis Research Center. Tests were conducted to 537 Kw (720 hp) at 14400 rpm. The effects of various operating conditions on spiral bevel gear steady state and transient temperature are presented. Also, a three-dimensional analysis of the thermal behavior was conducted using a nonlinear finite element analysis computer code. The analysis was compared to the experimental results attained in this study. The results agreed well with each other for the cases compared and were no more than 10 percent different in magnitude.

14. SUBJECT TERMS

Gears; Gear teeth; Transmissions

15. NUMBER OF PAGES

21

16. PRICE CODE

A03

17. SECURITY CLASSIFICATION OF REPORT	18. SECURITY CLASSIFICATION OF THIS PAGE	19. SECURITY CLASSIFICATION OF ABSTRACT	20. LIMITATION OF ABSTRACT
Unclassified	Unclassified	Unclassified	

National Aeronautics and
Space Administration

Lewis Research Center
21000 Brookpark Rd.
Cleveland, OH 44135-3191